1521-009X/46/7/934–942$35.00
Drug Metabolism and Disposition

https://doi.org/10.1124/dmd.118.080457
Drug Metab Dispos 46:934–942, July 2018

Metabolism of a $5HT_6$ Antagonist, 2-Methyl-1-(Phenylsulfonyl)-4-(Piperazin-1-yl)-1H-Benzo[d]imidazole (SAM-760): Impact of Sulfonamide Metabolism on Diminution of a Ketoconazole-Mediated Clinical Drug-Drug Interaction

Aarti Sawant-Basak, R. Scott Obach, Angela Doran, Peter Lockwood, Klaas Schildknegt, Hongying Gao, Jessica Mancuso, Susanna Tse, and Thomas A. Comery

Pfizer Worldwide Research and Development, Pharmacokinetics, Dynamics and Metabolism (PDM), Cambridge, Massachusetts (A.S.-B.); Pfizer Worldwide Research and Development, Pharmacokinetics, Dynamics and Metabolism (PDM), Groton, Connecticut (R.S.O., A.D., H.G., S.T.); Pfizer Global Product Development, Groton, Connecticut (P.L.); Pfizer Worldwide Research and Development Pharmaceutical Sciences Chemical Research and Development, Groton, Connecticut (K.S.); Pfizer Worldwide Research and Development, Research Statistics, Cambridge, Massachusetts (J.M.); and Pfizer Neuroscience and Pain Research Unit, Worldwide Research and Development, Cambridge, Massachusetts (T.A.C.)

Received January 10, 2018; accepted April 9, 2018

ABSTRACT

SAM-760 [(2-methyl-1-(phenylsulfonyl)-4-(piperazin-1-yl)-1H-benzo[d]imidazole)], a $5HT_6$ antagonist, was investigated in humans for the treatment of Alzheimer's disease. In liver microsomes and recombinant cytochrome P450 (P450) isozymes, SAM-760 was predominantly metabolized by CYP3A (~85%). Based on these observations and an expectation of a 5-fold magnitude of interaction with moderate to strong CYP3A inhibitors, a clinical DDI study was performed. In the presence of ketoconazole, the mean C_{max} and area under the plasma concentration-time curve from time zero extrapolated to infinite time values of SAM-760 showed only a modest increase by 30% and 38%, respectively. In vitro investigation of this unexpectedly low interaction was undertaken using [^{14}C]SAM-760. Radiometric profiling in human hepatocytes confirmed all oxidative metabolites previously observed with unlabeled SAM-760; however, the predominant radiometric peak was an unexpected polar metabolite that was insensitive to the pan-P450 inhibitor 1-aminobenzotriazole. In human hepatocytes, radiometric integration attributed 43% of the total metabolism of SAM-760 to this non-P450 pathway. Using an authentic standard, this predominant metabolite was confirmed as benzenesulfinic acid. Additional investigation revealed that the benzenesulfinic acid metabolite may be a novel, nonenzymatic, thiol-mediated reductive cleavage of an aryl sulfonamide group of SAM-760. We also determined the relative contribution of P450 to the metabolism of SAM-760 in human hepatocytes by following the rate of formation of oxidative metabolites in the presence and absence of P450 isoform–specific inhibitors. The P450-mediated oxidative metabolism of SAM-760 was still primarily attributed to CYP3A (33%), with minor contributions from P450 isoforms CYP2C19 and CYP2D6. Thus, the disposition of [^{14}C]SAM-760 in human hepatocytes via novel sulfonamide metabolism and CYP3A verified the lower than expected clinical DDI when SAM-760 was coadministered with ketoconazole.

Introduction

Alzheimer's disease (AD) is a progressive neurodegenerative disorder characterized by a decline in cognitive and functional abilities. It is the most common cause of dementia, with limited standards of care. The current pharmacotherapy for AD involves acetylcholinesterase inhibitors (e.g., donepezil and rivastigmine), which increase cholinergic tone throughout the brain by inhibiting the catabolism of acetylcholine via the inhibition of esterase activity. Although not disease modifying, these cause symptomatic relief and improvement of cognition over the shorter-term treatment. Therefore, adjunct therapies targeting receptors of complimentary mechanisms regulating the release of additional neurotransmitters like glutamate and serotonin may provide a new mechanism to increase the therapeutic potential of donepezil. One of these targets gaining recent attention was the $5HT_6$ receptor, which is a G-protein–coupled receptor expressed in brain regions that is critical for cognitive functioning and is positively coupled to adenylate cyclase. Microdialysis

No potential conflicts of interest relevant to this article are reported.
https://doi.org/10.1124/dmd.118.080457.

ABBREVIATIONS: 1-ABT, 1-aminobenzotriazole; AD, Alzheimer's disease; aq, aqueous; $AUC_{0\text{-inf}}$, area under the plasma concentration-time curve from time zero extrapolated to infinite time; CH_3CN, acetonitrile; [^{14}C] SAM-760, radioactive carbon isotope labeled SAM-760; DDI, drug-drug interaction; EPI, enhanced product ion; f_{CL}, fraction of total clearance; fCL, SAM-760, fraction of total clearance of SAM-760; F_g, fraction escaping the gut; F_g', fraction escaping metabolism in the intestine in the absence or presence of inhibitor; f_m, fraction of (2-methyl-1-(phenylsulfonyl)-4-(piperazin-1-yl)-1H-benzo[d]imidazole) metabolized by specific cytochrome P450 isoforms; GSH, glutathione; GST, glutathione transferase; HCOOH, formic acid; HLM, human liver microsome; HPLC, high-performance liquid chromatography; $5HT_6$, serotonin receptor subtype 6; IS, internal standard; LC, liquid chromatography; MeOH, methanol; MRM, multiple reaction monitoring; MS/MS, tandem mass spectrometry; *m/z*, charge/mass ratio; P450, cytochrome P450; PK, pharmacokinetic; Rt, retention time; SAM-760, (2-methyl-1-(phenylsulfonyl)-4-(piperazin-1-yl)-1H-benzo[d]imidazole); WEM, Williams' E medium.

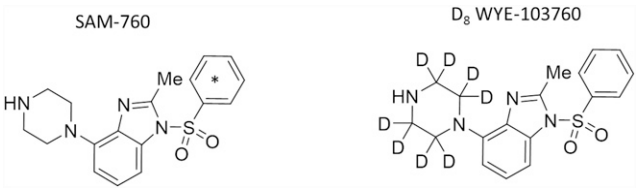

Fig. 1. Chemical structures of [^{14}C]SAM-760 and [D_8]WYE-103760.

in the rat cortex and hippocampus has shown that 5-HT_6 receptor antagonism stimulates extracellular acetylcholine and glutamate release, enhances cognition, and improves memory deficits in rodent models (Hirst et al., 2006; Foley et al., 2008). Early-stage clinical trials had illustrated the potential application of 5-HT_6 antagonists as an adjunct to donepezil in symptomatic treatment of AD (Maher-Edwards et al., 2011). Consistent with this rationale, drug design efforts led to the identification of SAM-760 [(2-methyl-1-(phenylsulfonyl)-4-(piperazin-1-yl)-1H-benzo[d]imidazole)] (Haydar, 2009; Liu et al., 2011) (Fig. 1), as a potential clinical 5-HT_6 antagonist, with projected efficacy at 50 mg/day. Prior to the administration of SAM-760 in humans, preliminary investigation of its major clearance mechanisms suggested that the main route of clearance was via oxidative metabolism of the piperazine core, including *N*-dealkylation. Substrate depletion kinetics of SAM-760 using human liver microsomes (HLMs) and recombinant cytochrome P450 (P450) isozymes showed that metabolic clearance was predominantly (~85%) via CYP3A. Therefore, during phase 1 clinical development, the effects of ketoconazole, a strong CYP3A inhibitor, were studied on the pharmacokinetic (PK) parameters of SAM-760. This clinical drug-drug interaction (DDI) study showed a 1.38-fold increase in plasma $AUC_{0\text{-inf}}$ values of SAM-760, in the presence of ketoconazole. This low magnitude of PK interaction was unexpected based on a fraction of SAM-760 metabolized by specific CYP isoforms (f_m) value of ~0.85. As a result, a deeper investigation of the clearance mechanisms of SAM-760 was conducted using radiolabeled material in a comprehensive metabolic system (i.e., human hepatocytes). This article describes the results of this investigation of [^{14}C]SAM-760. We report a previously unreported aryl sulfonamide cleavage pathway of SAM-760, which was subject to further mechanistic investigation. In addition, we also determined the exact contribution of CYP3A via metabolite formation kinetics in human hepatocytes using P450 isozyme–specific inhibitors to verify CYP3A victim DDI. This research exemplifies the importance of using radiolabeling compounds for deeper investigational studies of low-turnover compounds and the use of complete in vitro systems toward the accurate prediction of disposition- and victim-based DDIs of new clinical candidates.

Materials and Methods

[^{14}C]SAM-760 was synthesized as described below. SAM-760 was synthesized at Pfizer Research Laboratories (Haydar, 2009). WYE-103760 D_8 was obtained from Wyeth Research Laboratories (Pearl River, NY). Cryopreserved human hepatocytes (lot RTH) prepared as a mixture of 10 donor livers (seven females and three males) were purchased from Celsis InVitro Technologies (Baltimore, MD). All solvents and buffers were of high-performance liquid chromatography (HPLC) grade and were procured from J.T. Baker (Pittsburgh, PA). Furafylline, 1-aminobenzotriazole, ticlopidine, and mibefradil were purchased from Sigma-Aldrich (St. Louis, MO). Paroxetine was obtained from Sequoia Research Products (Pangborne, UK), and tienilic acid from Xenotech (Kansas City, KS). All other reagents were of the highest grade commercially available. All clinical studies were conducted in compliance with the ethical principles originating in or derived from the Declaration of Helsinki and were in compliance with all International Conference on Harmonization Good Clinical Practice Guidelines and the International Ethical Guidelines for Biomedical Research Involving Human Subjects (Council for International Organizations of Medical Sciences, 2002). All local regulatory requirements were followed, in the interest of greater protection to the safety of study participants.

Synthesis of [^{14}C]SAM-760

Preparation of [^{14}C]*t*-Butyl 4-(2-methyl-1-(phenylsulfonyl)-1H-benzo[*d*]-imidazol-4-yl)piperazine-1-carboxylate (2). A solution of **1** (593 mg, 1.87 mmol) and Hünig's base (0.39 ml, 2.25 mmol) in 4 ml of isopropyl acetate was treated with a solution of [^{14}C]benzenesulfonyl chloride (150 mCi, 80 mCi/mmol, 1.87 mmol) in 2 ml of isopropyl acetate. The reaction was heated at 65°C for 2 hours, and then cooled to room temperature and partitioned between 5 ml of water and 5 ml of isopropyl acetate. The organic layer was washed with 5 ml of water and concentrated to afford an oil. The oil was diluted with 3 ml of isopropyl acetate and 6 ml of heptane and seeded at room temperature with nonlabeled **2**. The resulting suspension was cooled to 0°C and filtered, rinsing with heptane. The collected product was air dried to give **2** (564 mg, 1.23 mmol, 66% yield) as a white solid.

Preparation of [^{14}C]SAM-760. A suspension of **2** (564 mg, 1.23 mmol) in 3 ml of toluene was cooled to 0°C and treated with trifluoroacetic acid (0.95 ml, 12.3 mmol). The resulting biphasic mixture was stirred at room temperature for 2.5 hours. A mixture of concentrated ammonium hydroxide (1.7 ml, 12.3 mmol) in 10 ml of isopropyl acetate was added, and the reaction was stirred for an additional 2 hours. The resulting biphasic mixture was treated with 5 ml of 5% aqueous (aq) K_2CO_3, and the layers were separated. The organic layer was washed with 5 ml of 5% aq K_2CO_3 followed by 2 × 10 ml of water. The organic layer was concentrated to afford an oil, and this was diluted with 2 ml of isopropyl acetate and 3.5 ml of heptane. The resulting suspension was cooled to 0°C and filtered, rinsing with heptane. The collected product was air dried to give [^{14}C]SAM-760 (324 mg, 0.90 mmol, 73% yield) as a white solid A summary of radiolabeled synthesis is depicted in Scheme 1.

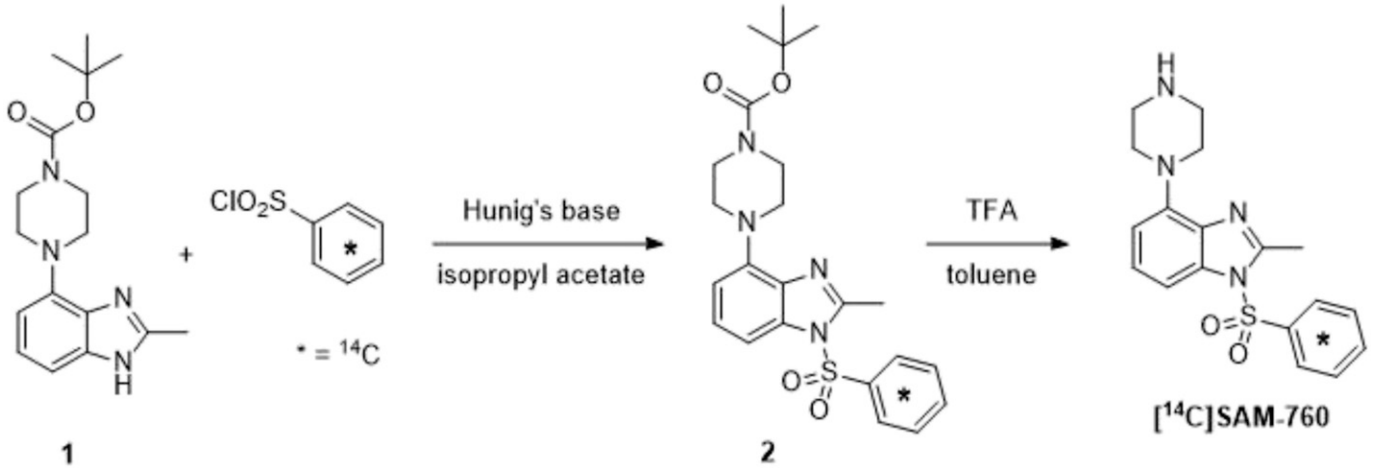

Incubation of [^{14}C]SAM-760 in Human Hepatocytes for Metabolite Identification in Presence and Absence of 1-ABT. Hepatocytes were thawed as per the supplier protocol. Thawed hepatocytes were suspended in Williams' E medium (WEM), and cells were counted for viability, using the Trypan blue exclusion method. After meeting an internal acceptance criteria of >85% viability of the total number of cells, the hepatocyte suspension was diluted in WEM to achieve the desirable cell concentration (i.e., 0.75 million cells/ml). A mixture of radiolabeled SAM-760 ([^{14}C] SAM-760, 6.7 mCi/mmol) and unlabeled SAM-760 (10 μM) was incubated with cryopreserved human hepatocytes diluted to 0.75 million cells/ml in WEM at 37°C under an atmosphere of 95% O_2/5% CO_2 and in a final incubation volume of 1.5 ml. Samples were shaken on a rotating platform at 200 rpm in an incubator. P450 metabolism was quantitatively assessed by conducting incubations of SAM-760 in cryopreserved hepatocytes in the presence or absence of the pan-CYP inhibitor 1-ABT. Experiments containing 1-ABT were conducted by a 30-minute preincubation of cryopreserved hepatocytes with 1-ABT prior to the addition of 10 μM SAM-760. Incubations were terminated by the addition of 50 μl of 0.1% HCOOH after 0 and 4 hours The mixtures were centrifuged, and supernatants were analyzed using HPLC followed by radiometry and mass spectrometry (see below). Incubations were performed in triplicate.

HPLC-Mass Spectrometry and Radiometric Analysis of [^{14}C] SAM-760. Terminated incubation mixtures were injected (0.1 ml) onto a Varian Polaris C_{18} column (4.5 × 250 mm; 5 μm) in a mobile phase consisting of 0.1% HCOOH in CH_3CN (10%) at a flow rate of 0.8 ml/min. This composition was maintained for 5 minutes followed by a linear gradient to 50% CH_3CN at 50 minutes, a 10-minute wash in 95% CH_3CN, and a 10-minute re-equilibration time under the initial conditions. The effluent was split between a fraction collector and an LTQ Ion Trap Mass Spectrometer (Thermo Fisher Scientific; Waltham, MA) (split ratio was ~1:15). The mass spectrometer was operated in the positive ion mode, with tuning parameters and potentials optimized to maximize the signal for the protonated molecular ion of SAM-760. Fractions were collected every 20 seconds into a 96-well Scintiplates (PerkinElmer, Waltham, MA) and subjected to vacuum centrifugation to remove the solvent. The dried plates were counted in a MicroBeta Scintillation Counter (PerkinElmer) (3-minute counting time). The radiochromatograms from individual incubations were averaged; the percentage of each of the metabolites was calculated by manual integration of the averaged radiometric peaks of individual metabolite and normalized to total radioactivity in the incubations.

Inhibition of SAM-760 Metabolism in Human Hepatocytes Using P450 Isozyme-Specific Inhibitors. In a preliminary experiment, it was shown that the metabolite profile at substrate concentrations of 1 and 10 μM was the same and that there was an approximately 10-fold greater abundance of all metabolites of SAM-760 at 10 versus 1 μM. Therefore, all subsequent experiments were carried out at a substrate concentration of 10 μM. Thus, SAM-760 (10 μM) was incubated with cryopreserved human hepatocytes (0.75 million cells/ml) in the presence or absence of P450-selective inhibitors. The incubations (N = 3) were conducted in 24-well cell culture plates at 37°C in a CO_2 incubator under an atmosphere of 95% O_2/5% CO_2. Human hepatocytes were preincubated for 30 minutes with P450-selective time-dependent inactivators of CYP1A2 (1 μM furafylline), CYP2C9 (10 μM tienilic acid), CYP2C19 (30 μM ticolpidine), CYP2D6 (2 μM paroxetine), and CYP3A4/5 (10 μM mibefradil) prior to the addition of SAM-760. The reactions were terminated after 1 hour of incubation by transferring aliquots to a clean 96-well plate and centrifuging for 3 minutes at 50g. The resulting supernatants were transferred to a clean 96-well plate containing internal standard (IS) (250 ng/ml metoprolol and terfenadine) and were stored at −80°C prior to analysis.

Semiquantitative Analysis of Metabolites in Chemical Inhibition Samples, Using HPLC-Tandem Mass Spectrometry. Liquid chromatography (LC) separation was performed on a Kinetex C-18 (Phenomenex, Torrance, CA) (2.1 × 50 mm, 107 μm) coupled to an Acquity UPLC system (Waters, Milford, MA). The mobile phase B was acetonitrile, and the aq mobile phase A was prepared with HCOOH at 0.1% concentration. The flow rate for all experiment was 0.5 ml/min. The sample was injected using a linear gradient of 2% phase B (0.1% HCOOH/acetonitrile) with an Aquity Autosampler (Waters) with a 5.0-μl injection volume for a total run time of 3 minutes. Chemical inhibition samples were injected (5.0 μl) onto a Phenomenex Kinetex C-18 column (2.1 × 50 mm, 1.7-μm) in an initial mobile phase composition of 98% of 0.1% HCOOH in water (phase A), and 2% of 0.1% HCOOH in acetonitrile (phase B) at a flow rate of 0.5 ml/min for 0.5 minute. This was followed by consecutive linear gradients of 1.5 minutes to 60% phase B and then 18 seconds to 90% phase B, where it was held for 12 seconds An 18-second linear gradient returned the column to the initial composition where the column was re-equilibrated for 12 seconds Mass spectrometric semiquantitative experiments were performed on an API5500 QTRAP Mass Spectrometer (AB Sciex, Framingham, MA) in the positive electrospray ionization mode. Semiquantitative methods for quantitating P450-sensitive metabolites in chemical inhibition studies were developed by injecting samples generated from a pilot study where unlabeled SAM-760 was incubated with hepatocytes. The metabolites generated in this pilot experiment were determined using multiple ion monitoring-enhanced product ion (EPI) scans to qualitatively confirm the identity and establish the retention time of the metabolites relative to those observed in the biotransformation studies with radiolabeled material. Product ions were generated for the most intense parent ion with a response greater than 5000 cps after dynamic background subtraction. A semiquantitative multiple reaction monitoring (MRM)-EPI method was then created for sample analysis by linking the parent ion with the most intense product ion. MRM responses greater than 5000 cps after dynamic background subtraction triggered EPI scans to qualitatively confirm the identification of the metabolite, and MRM metabolite/IS peak area ratios were used to determine the percentage of inhibition. Triggered EPI scans were collected at collision energies of 50, 40, and 30 eV with a scan rate of 20,000 Da/s. The MRM transitions and retention times of the analytes are listed in Table 2. The following mass-independent, mass spectrometer parameters were applied to detect SAM-760 and the following test compounds: collision energy, 35 eV for MRM transitions; declustering potential, 50 V; temperature, 450°C; IS voltage, 4500 V; dwell time, 2.0 milliseconds; and collision gas set at medium. Analyst version 1.5.1 (AB Sciex) was used to control the LC-tandem mass spectrometry (MS/MS) system, collect data, and perform data reduction. Since the measured metabolites would be in a linear dynamic range, this semiquantitative method was considered to be adequate for measuring metabolites from the chemical inhibition study.

Data Analysis

To estimate the overall contribution of individual P450 enzymes to the overall metabolism of SAM-760, a three-step process was conducted. First, the fraction of overall metabolism of [^{14}C]SAM-760 to each individual metabolites was calculated from the radiochromatogram data as follows in eq. 1:

$$\frac{\text{radioactivity in metabolite X peak}}{\text{total radioactivity in chromatogram}} = f_{CL(\text{metabolite X})} \quad (1)$$

Next, the LC-MS-MS peak area ratios of each of the metabolites in chemical incubations (of unlabeled SAM-760 in human hepatocytes with and without specific P450 inhibitors) were determined. The fraction of control for a metabolite X using an inhibitor of "CYP #1" was calculated in eq. 2 by the following:

$$\frac{\text{peak area of metabolite X in presence of inhibitor}}{\text{peak area of metabolite X in no inhibitor control}} = f_{\text{control(metabolite X, CYP\#1)}} \quad (2)$$

Then, the contribution of CYP#1 to the total metabolism of SAM-760 was calculated by summing the metabolic contributions of all metabolites generated by CYP#1 as follows in eq. 3:

$$f_{CL,\text{SAM-760(P450\#1)}} = f_{CL(\text{metabolite X})} \bullet f_{\text{control(metabolite X, P450\#1)}} + f_{CL(\text{metabolite Y})} \bullet f_{\text{control(metabolite Y, P450\#1)}} + \cdots\cdots\cdots \quad (3)$$

Thus, the f_m were determined by integrating results from chemical inhibition studies into the HPLC-radiochromatographic measurements. The fraction of clearance determined was converted to the percentage contribution of individual P450 inhibitors.

Incubation of SAM-760 with Thiols. SAM-760 (200 μM) was incubated with glutathione (GSH) (5 mM), *N*-acetyl cysteine (5 mM), β-mercaptoethanol (100 mM), or no thiol (control) in 1 ml of 100 mM potassium phosphate at pH 7.5 and 37°C. These reaction mixtures were directly injected (0.02 ml) onto a Waters HSS T3 UHPLC Column (2.1 × 100 mm; 1.7 μ) equilibrated in 10 mM aq ammonium acetate at a flow rate of 0.4 ml/min. This mobile phase condition was held for 0.5 minute followed by a linear increase to 80% acetonitrile at 5 minutes,

was held for 1 minute, and was re-equilibrated to initial conditions for 1 minute. The effluent was introduced into a Orbitrap Elite High-Resolution Mass Spectrometer (Thermo Fisher Scientific) operated in the negative ion full MS1 scan mode. Source temperatures and potentials were adjusted to optimize the signal for benzenesulfinic acid, which eluted at 2.7 minutes.

Human Plasma PKs of Oral SAM-760 Administered with or without Ketoconazole. On day 1, period 1, comprising (N = 12) healthy, young, male subjects, received a single 5-mg dose of SAM-760 was administered after an overnight fast of at least 10 hours. In period 2, from day −2 to day 12 (a total of 14 days), each subject received a daily dose of ketoconazole 400 mg every day (2 × 200 mg tablets). In period 2, day 12, a single 5-mg dose of SAM-760 was coadministered (with ketoconazole) after an overnight fast of at least 10 hours. Blood samples (5 ml) were obtained −1, 0.5, 1, 1.5, 2, 3, 4, 6, 8, 10, 12, 16, 24, 36, 48, 72, and 96 hours after SAM-760 administration and centrifuged. EDTA plasma was harvested by centrifugation (3000g for 10 minutes) of whole blood at 4°C. Samples were stored at −20°C until further processing or analysis.

Quantification of SAM-760 in Human Plasma. A validated LC-MS/MS method quantitated SAM-760 in human EDTA plasma. The method used an automated solid-phase extraction procedure prior to LC-MS/MS analysis. A stable isotope-labeled version of SAM-760, WYE-103760 D_8 (Fig. 1), was used as the IS. The linearity of SAM-760 in human plasma was observed over the concentration range of 0.250–500 ng/ml, using a plasma sample volume of 0.100 ml. Reconstituted extracts of EDTA plasma were analyzed by LC-MS/MS. A 5-minute gradient was used to achieve separation using an API 4000 System (Applied Biosystems, Foster City, CA) using a binary pump to deliver mobile phase. Extracts were injected (10 μl) onto an Echelon C-18 column (30 × 2.1 mm, 4 μM), equilibrated in 10% MeOH/10% ACN/80% H_2O/0.1% HCOOH at a flow rate of 0.4 ml/min for 0.5 minute, followed by a change in gradient from 0.5 to 1.6 minutes to 40% MeOH/50% ACN/10% H_2O/0.1% HCOOH (v/v). The gradient was held from 1.6 to 3.8 minutes and then equilibrated to starting conditions from 3.8 to 5 minutes. SAM-760 and IS were detected in positive ion electrospray using MRM mass transitions for SAM-760 (m/z 357.16 → 216.15) and IS (m/z 365.12 → 224.10). The dynamic range of the assay was from 0.05 to 1000 ng/ml. Peak-area integrations were performed using AB Sciex/Applied Biosystems Analyst software (version 1.4.2 or successor system).

PK Calculations. PK parameters of SAM-760 were derived from a plasma concentration versus time profile. Plasma PK parameters of SAM-760 (C_{max} and $AUC_{0\text{-inf}}$) were calculated using version 2.2.2 eNCA, which is a Pfizer proprietary global repository for PK concentration and NCA parameter data as well as the global system for generating noncompartmental analyses. Samples below the lower limit of quantitation (0.25 ng/ml) were set to 0 ng/ml for data analysis.

Results

Metabolism of [^{14}C]SAM-760 in Cryopreserved Human Hepatocytes. [^{14}C]SAM-760 (labeled on the aryl ring system, Fig. 1) was incubated in human hepatocytes for t = 0 (control) and t = 4 hours. The incubation mixtures were assessed using HPLC followed by radiometric assessment as well as mass spectrometry, and are depicted in Fig. 2 as blue (control) and red (t = 4 hours) traces. The green trace in Fig. 2 represents [^{14}C]SAM-760 (10 μM) incubated with human hepatocytes and 1 mM 1-ABT. SAM-760 showed a slow rate of metabolism in human hepatocytes over 4 hours of incubation as observed from the radiochromatogram (Fig. 2, red trace), where the largest radioactive peak belonged to the parent compound (R_t, ~35 minutes). The peaks eluting at R_t at ~14 and ~26 minutes (designated with "i" in Fig. 2) represent radiochemical impurities and were not included in data analysis. Metabolite peaks observed in this radiometric HPLC analysis have been designated as peaks 1–15, and their proposed structures are shown in Fig. 3 and are described below; wherever possible, metabolites were confirmed by coelution with authentic standards, which were biosynthesized (methods not shown) or commercially purchased.

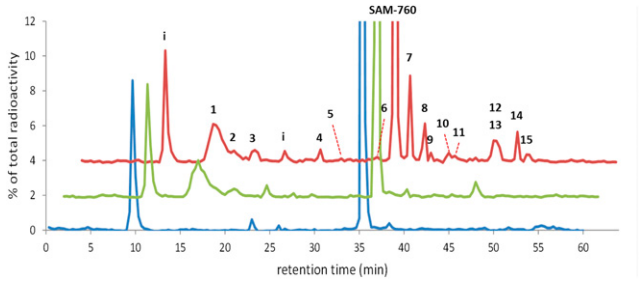

Fig. 2. HPLC radiochromatograms of metabolites of [^{14}C]SAM-760 in human hepatocyte incubations. [^{14}C]SAM-760 (10 μM) was incubated with human hepatocytes for 4 hours without (red top trace) or with (green middle trace) 1 mM 1-ABT. The blue bottom trace is a control incubation at t = 0 hour. Numbers designate the individual metabolites listed in Table 1. Peaks designated with "i" represent radiochemical impurities, and the large peak eluting at ~35 minutes is the unchanged parent drug (SAM-760).

Several drug metabolism reactions contributed to the 15 metabolite peaks observed from the incubation of [^{14}C] SAM-760 in human hepatocytes. Peaks arose via hydroxylation, N-oxidation, piperazine oxidation, N-sulfation, and reductive sulfonamide cleavage (Fig. 3). Peak 1, which was broad and polar (eluted earlier than the parent, on the C-18 column; R_t, ~15 minutes), was the most abundant metabolite peak, and was of significant interest because it represented the predominant metabolic pathway of SAM-760 in human hepatocytes. In positive ion electrospray, it corresponded to m/z 143 and fragmented to predominant daughter ions of m/z 125 and m/z 79, corresponding to a loss of water molecule and 64 atomic mass units, respectively. Although the peak of m/z 125 did not reveal significant information, the loss of 64 atomic mass units from m/z 143 was suggestive of a loss of $-SO_2$ from the molecule; the resulting stable daughter ion of m/z 79 corresponded to a benzylium species, further suggesting that m/z 143 could be benzenesulfinic acid arising from the aryl sulfonamide moiety of SAM-760. Based on an m/z of 143 and coelution of peak 1 with an authentic standard, it was confirmed to be benzenesulfinic acid (Fig. 4). Peaks 2 and 4 were present at 6.3% and 1.9% of metabolism, respectively, but were not identified, as no mass spectral data were observed for either of them.

Almost all of the remaining peaks arose via oxidation reactions, including hydroxylation on the benzimidazole ring (peaks 5 and 6), N-hydroxylation of the 2° piperazine nitrogen (peak 9), and oxidative ring–opening reactions of the piperazine (peaks 7, 11, 14, and 15). Peak 3 was identified as the glucuronidated conjugate of peak 5/6, and peak 13 was proposed to be an N-acetyl conjugate of the piperazine ring oxidation product. Peak 12 was identified as the sulfamic acid conjugate of the 2° piperazine nitrogen. In conclusion, SAM-760 metabolized to several primary and secondary metabolites when incubated in human hepatocytes; the predominant pathway of metabolism was identified as cleavage of the imidazole sulfonamide, forming benzenesulfinic acid.

Contribution of P450-Mediated and Non-P450–Mediated Metabolism of ^{14}C SAM-760 in Human Hepatocytes. The formation of benzenesulfinic acid and its contribution to total metabolic clearance was determined by the incubation of [^{14}C]SAM-760 in the presence (green trace) and the absence of 1 mM 1-ABT (red trace) as shown in Figure 2. The formation of peak 1 was not sensitive to the presence of 1 mM 1-ABT, demonstrating that this was a non-P450–mediated clearance mechanism. The contribution of each metabolic pathway (percentage of metabolism) to the overall clearance of SAM-760 was determined by dividing the radiometric response of an individual metabolite by the sum of all drug-related radiometric metabolite peaks identified in the study. The benzenesulfinic acid metabolite was calculated to be 43% of total metabolism, further confirming that it was indeed the major biotransformation route of clearance of SAM-760. After quantitating the sulfinic acid metabolite, all other metabolites represented between 1 and 12 were calculated as the percentage of total metabolism. Among the remaining routes of clearance, the piperazine sulfamic acid metabolite

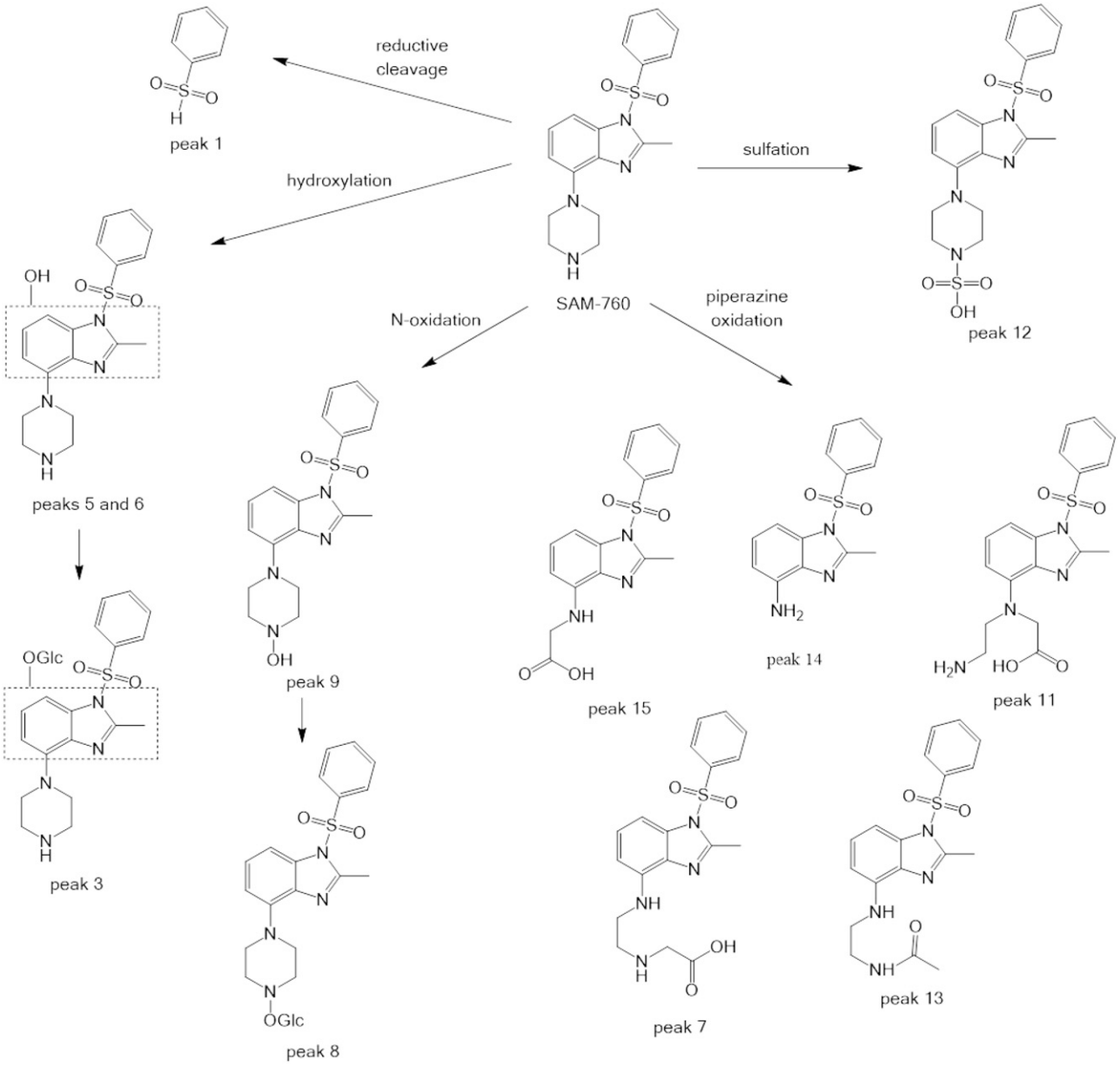

Fig. 3. Proposed metabolic pathways of SAM-760 observed in human hepatocytes.

was attributed to be 4.5% of total metabolic clearance, suggesting that the remaining ~40%–45% of metabolic clearance could be mediated by P450 (Table 1).

P450 Reaction Phenotyping in Human Hepatocytes Using P450-Specific Inhibitors. As determined above, P450-mediated metabolism contributed to ~40%–45% of total metabolic clearance (Table 1). The contribution of CYP3A toward the total P450-mediated metabolism of SAM-760 was determined by the incubation of SAM-760 in human hepatocytes in the presence or absence of P450-selective inhibitors. To determine the CYP contribution to each specific metabolic pathway of SAM-760 in human hepatocytes, the relative change in metabolite formation in the presence or absence of a P450-selective inhibitor was calculated using eq. 1, 2, 3. Incubation of SAM-760 in human hepatocytes in the presence or absence of P450-selective inhibitors ticlopidine, paroxetine, and mibefradil indicated that CYPC19, CYP2D6, and CYP3A4/5 contributed to the P450-mediated metabolism of SAM-760. There were no inhibitory effects on the formation of any of the metabolites by furafylline (CYP1A2 inactivator) or tienilic acid (CYP2C9 inhibitor). Inhibition by mibefradil was observed on peaks 3, 8, 9, 13, 14, and 15. In addition to mibefradil, peaks 6, 7, 10, and 11 were also inhibited by ticlopidine; peak 5 was inhibited by paroxetine. Results are summarized in Table 2. In human hepatocytes, the oxidative metabolism of SAM-760 was predominantly attributed to CYP3A (33%), with minor contributions by CYP2C19 (6.3%) and CYP2D6 (0.47%). P450-mediated metabolism accounted for up to 39.8% of the total clearance pathways of SAM-760, with CYP3A playing a major role in oxidative metabolism.

Incubation of SAM-760 with Thiol Reagents. Two hundred micromolar SAM-760 was incubated in buffer (pH 7.5) with GSH (5 mM), *N*-acetyl cysteine (5 mM), β-mercaptoethanol (100 mM), or no thiol (control). Incubations were injected onto LC-MS/MS under negative ion electrospray ionization. The presence of benzenesulfinic

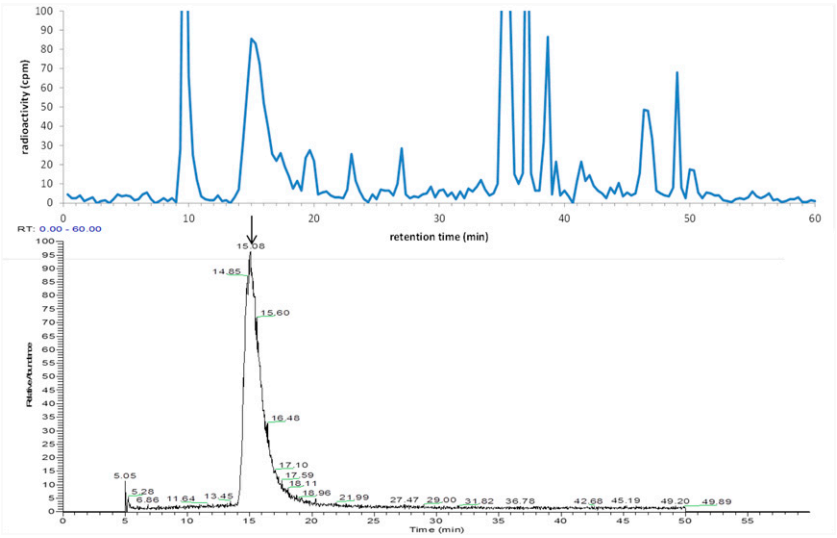

Fig. 4. Comparison of elution profile of benzenesulfinic acid under identical chromatographic conditions. Top panel shows benzenesulfinic acid as observed in the radiochromatogram of SAM-760, on incubation of [^{14}C] SAM-760 in human hepatocytes. Bottom panel is the extraction ion chromatogram of benzenesulfinic acid (under negative ion chromatogram of *m/z* 141). Arrows indicate the corresponding peaks at ~15 minutes.

acid in incubations containing a thiol but not in the control was observed (Fig. 5). This suggested that the observation of benzenesulfinic acid in hepatocyte incubation of SAM-760 likely arises by chemical reduction of the aryl sulfonamide bond of SAM-760 by GSH or other thiols present in the incubations.

PK Parameters of SAM-760 in Healthy Volunteers in Presence and Absence of Ketoconazole. Healthy male volunteers were administered a single oral dose of SAM-760 (5 mg) alone or with ketoconazole (400 mg). Mean exposures of SAM-760 after a single 5-mg oral dose (C_{max}, 3.43 ng/ml; $AUC_{0\text{-inf}}$, 154.5 ng/h per milliliter) increased (C_{max}, 4.47 ng/ml; $AUC_{0\text{-inf}}$, 213.7 ng/h per milliliter), when it was coadministered with ketoconazole (Fig. 6; Table 3). Thus, in the presence of ketoconazole, the mean plasma C_{max} and $AUC_{0\text{-inf}}$ values of a single oral dose of 5 mg of SAM-760 increased by 30% and 38%, respectively.

Discussion

Prior to the administration of a new drug candidate to humans, DDIs (the inhibition of clearance pathways of a compound resulting in increased exposure) could be predicted with reasonable confidence by integrating in vitro clearance estimations and the fraction metabolized or, less frequently, in vivo animal studies (Kotegawa et al., 2002; Vuppugalla et al., 2012). If there is high confidence that all human clearance pathways are recapitulated by the in vitro systems used, then the fundamental relationship to predict victim DDIs using static (eq. 4) or dynamic modeling (e.g., SimCYP) emphasizing F_g and $f_{m,CYPi}$, (Guest et al., 2011), can be applied

$$\frac{AUC'}{AUC} = \frac{F_G'}{F_G} \bullet \frac{1}{\sum_{i}^{n} \frac{fm_{CYP_i}}{1+\sum_{j}^{m} \frac{[I]_j}{K_{i,j}}} + \left(1 - \sum_{i}^{n} fm_{CYP_i}\right)} \quad (4)$$

where [I] is the inhibitor concentration, $K_{i,}$ is the inhibition constant, f_m is the fraction of substrate drug metabolized by P450 enzyme under investigation, $(1 - f_{m,CYPi})$ represents clearance via other P450 enzymes and/or renal clearance, F_g is the fraction escaping the gut, and F_g' represents the fraction escaping metabolism in the intestine in the absence or presence of inhibitor. Eq. 4 demonstrates the significance of f_m. Inaccuracy in f_m estimates could result in an underprediction of

TABLE 1

Summary of proposed metabolites observed in radiochromatogram (red trace in Fig. 2) and percentage of metabolism of SAM-760 in human hepatocytes

Peak Number	R_t (min)	*m/z*	Putative Identification	Total Radioactivity from Metabolites	1-ABT Sensitive?
	min			%	
1	15.2	143	Benzenesulfinic acid	43	No
2	~18	N.D.	Unknown	6.3	No
3	19.7	549	Glucuronide of peak 5	4.5	Yes
4	~27	N.D.	Unknown	1.9	Yes
5	30.1	373	Hydroxyl on methyl benzimidazole	1.3	Yes
6	33.0	373	Hydroxyl on methyl benzimidazole	1.5	Yes
SAM-760	35.1	357	SAM-760	N/A	N/A
7	36.7	389	Carboxylic acid	12	Yes
8	38.5	549	Glucuronide of peak 9	7.2	Yes
9	39.1	373	Hydroxylamine of piperazine	1.3	Yes
10	41.3	369	Unknown	2.0	Yes
11	41.8	389	Carboxylic acid	1.7	Yes
12	45.3	437	Sulfamic acid on piperazine	4.5	No
13	46.6	373	*N*-acetyl cysteine	4.8	Yes
14	48.8	288	Cleaved piperzine	5.8	Yes
15	50.0	346	Piperazine oxidation	2.6	Yes

N/A, not applicable; ND, not determined.

TABLE 2

Cumulative contribution of P450 isozymes, to each of the 1-ABT–sensitive metabolic pathways of SAM-760 in human hepatocytes, determined using eq. 1, 2, 3

Peak Number in Fig. 2	HPLC R_t (min)	MRM Transition	CYP2C19	CYP2D6	CYP3A
	min				
Peak 3	1.18	549 → 232			4.3%
Peak 5	1.46	373 → 232		0.47%	0.83%
Peak 6	1.53	373 → 174	0.06%		0.90%
Peak 7	1.66	389 → 160	4.5%		10%
Peak 8	1.69	549 → 232			3.3%
Peak 9	1.70	373 → 232			0.69%
Peak 10	1.91	369 → 228	0.85%		1.1%
Peak 11	1.91	389 → 248	0.80%		0.90%
Peak 13	2.0	373 → 232			3.4%
Peak 14	2.06	288 → 147.1			5.5%
Peak 15	H2.04	346 → 160.1			2.4%
SAM-760 fraction metabolized (f_m)	N/A	N/A	6.3%	0.47%	33%

N/A, not applicable.

victim interactions, leading to a higher than expected increase in exposure of the probe substrate and potential toxicological events; in contrast, an overprediction of the DDI may suggest an inaccuracy in the estimation of f_m and potential missed pathways of disposition of the investigational molecule. The current report discusses one such case study of how lower than predicted victim interactions of an investigational $5HT_6$ antagonist, SAM-760, led to a renewed assessment of the clearance pathways of this molecule using radiolabeled [^{14}C]SAM-760 in human hepatocytes. The metabolism of [^{14}C]SAM-760 (Fig. 1) in human hepatocytes revealed a previously unidentified and structurally unanticipated pathway, which was insensitive to the presence of 1-ABT. Subsequent enzyme mapping of the remaining, 1-ABT–sensitive metabolic disposition via product formation in human hepatocytes verified the magnitude of the CYP3A DDI of SAM-760 that was observed in the clinical DDI study in the presence of ketoconazole.

SAM-760 was identified as a potent $5HT_6$ antagonist suitable for clinical development. In HLMs, under standard incubation conditions, SAM-760 demonstrated low metabolic turnover and was primarily oxidatively metabolized at the piperazine ring. Substrate depletion experiments of SAM-760 in recombinant P450 isozymes and in HLMs using P450-specific inhibitors suggested that CYP3A was the predominant metabolic isozyme, contributing to ~85% of metabolic clearance. Using ketoconazole as the probe CYP3A inhibitor, the static equation predicted an ~5-fold change in plasma $AUC_{0\text{-inf}}$ of SAM-760, suggesting a high likelihood of significant interaction with moderate to strong CYP3A inhibitors. However, in a clinical DDI study when SAM-760 (5 mg, by mouth) was coadministered with ketoconazole (400 mg, by mouth), a modest 1.38-fold increase in mean plasma C_{max} and $AUC_{0\text{-inf}}$ levels of SAM-760 was observed (Fig. 6; Table 3).

This 1.38-fold PK interaction of SAM-760 with ketoconazole was inconsistent with the predicted (~5-fold) change. The lower than predicted interaction with ketoconazole obviated the need to exclude concomitant drugs that may be moderate to strong CYP3A inhibitors. However, this unexpected clinical data suggested that CYP3A may not be the predominant pathway of clearance of SAM-760, and that substrate depletion experiments of unlabeled SAM-760 in HLMs may have overestimated its CYP3A contribution. These data also suggested a potential role of additional, non-P450–mediated clearance mechanisms of SAM-760. An understanding of all the clearance pathways is an important consideration for defining inclusion and exclusion criteria in later phases of clinical programs.

Therefore, additional investigation was undertaken using radiolabeled [^{14}C]SAM-760, with the label located on the aryl ring adjacent to the sulfonamide group (Fig. 1). The position of the label had been selected due to the absence of metabolic events on the aryl ring, during incubations of unlabeled SAM-760 in liver microsomes. Due to the low turnover of SAM-760 in HLMs and to identify any other missed pathways of metabolism, experiments using [^{14}C]SAM-760 (Fig. 1)

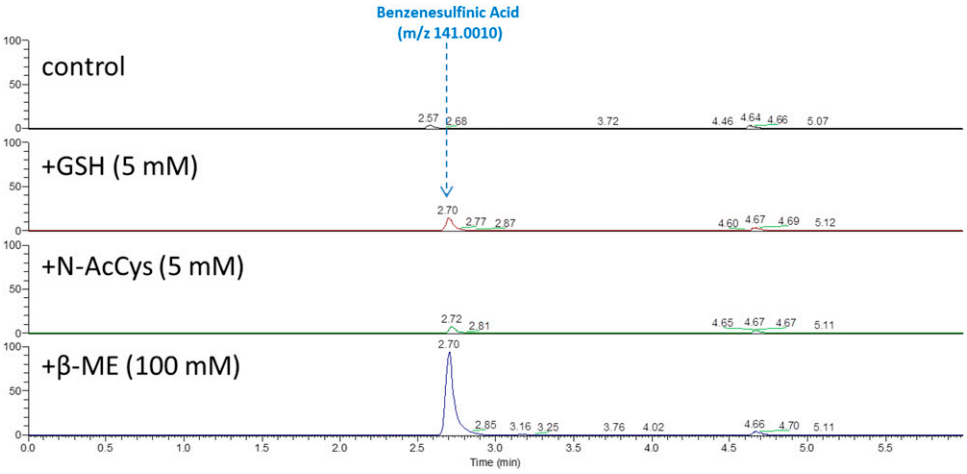

Fig. 5. Negative ion electrospray extracted ion chromatograms of benzene sulfonate ion (*m/z* 141). The panels (top to bottom) are XICs (extracted ion chromatogram) from incubation of SAM-760 in buffer with no thiols added (control), GSH, *N*-acetyl cysteine, and β-ethanethiol.

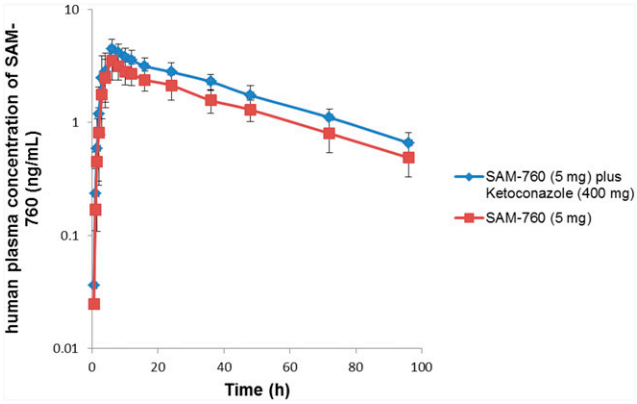

Fig. 6. Mean ± S.E.M. plasma concentrations of SAM-760 after a single oral 5-mg dose (red trace) or after 400 mg ketoconazole administered daily for 2 weeks (blue trace).

were undertaken in a more comprehensive metabolic system of cryopreserved human hepatocytes; incubates were analyzed using HPLC followed by radiochromatography and MS/MS. Radiochromatograms of [^{14}C]SAM-760 incubated in human hepatocytes attributed the highest radioactivity to an unexpected, new, high-abundance, broad, highly polar metabolite eluting much earlier than the parent molecule, at ~15.2 minutes, and corresponding to an *m/z* 143. Exact mass measurements and fragmentation patterns revealed that this polar metabolite may be benzenesulfinic acid, potentially originating from the metabolism of the aryl sulfonamide of SAM-760 (Fig. 4). In human hepatocytes, this peak contributed to ~43% of the total radioactivity attributed to metabolites of SAM-760 and was insensitive to 1-ABT (Fig. 2; Table 1); remaining metabolites were inhibited by 1-ABT.

This observation of benzenesulfinic acid to be the predominant metabolic pathway in human hepatocytes was consistent with a separate investigation of [^{14}C]SAM-760 in a rat mass balance study. This study also showed that metabolic clearance predominated via biotransformation of the aryl sulfonamide; <10% of total radioactivity was attributed to unchanged SAM-760 in urine and feces, confirming that renal and biliary pathways were minor routes of elimination of SAM-760 (data not shown). Overall, the predominance of this non-CYP3A–mediated metabolic clearance of SAM-760 may explain the lack of significant DDI with ketoconazole in the clinical DDI study.

The metabolism of the aryl sulfonamide benzimidazole group to benzenesulfinic acid was unanticipated and unprecedented. This is intriguing since sulfonamides are metabolically and chemically stable. It has been reviewed shown in a review article (Kalgutkar et al., 2010) that the metabolism of a sulfonamide is not as straightforward as that of amides and esters, and requires *N*-hydroxylation as a rate-limiting step, under strongly alkaline or anaerobic conditions, resulting in subsequent release of NO^{+} radical and sulfonic acid metabolite. However, this opportunity does not exist for SAM-760 due to the unavailability of an alpha proton on the benzimidazole nitrogen that constitutes the sulfonamide core. The cleavage of activated sulfonamides by nucleophilic attack of GSH in the presence of GSTs and *N*-acetyl transferases has been reported previously; cleaving of sulfonamides via the activation of sulfonamides has been applied as a prodrug strategy for metformin (Larsen and Bundgaard, 1989; Singh et al., 2006; Rautio et al., 2014). GST-catalyzed displacement of PNU-109112 has been reported and the structure-metabolism relationship of activated sulfonamides has been studied (Koeplinger et al., 1999; Zhao et al., 1999). Similarly, GSH- or cysteine-mediated nucleophilic displacement of hetero-aryl–substituted sulfonamides has also been reported (Conroy et al., 1984). However, our investigation did not support nucleophilic displacement of the aryl sulfonamide from the benzimidazole-sulfonamide group of SAM-760 because no GSH or *N*-acetyl cysteine conjugates of SAM-760 or of its metabolites were observed. Incubation of SAM-760 with GSH in the presence of human GST did not form benzenesulfinic acid or GSH/*N*-acetyl cysteine conjugates of SAM-760. On the contrary, control incubations of SAM-760 with GSH (no GST added) showed small amounts of benzenesulfinic acid. We proposed that the metabolism of SAM-760 to benzenesulfinic acid may progress nonenzymatically and may be a reduction mediated by thiols like GSH. We confirmed this hypothesis by a subsequent incubation of SAM-760 with the following three different thiols: GSH, *N*-acetyl cysteine, and β-ethanethiol (Fig. 5). Human hepatocytes contain endogenous thiols like cysteine and GSH. Thus, it can be hypothesized that under the incubation conditions described above, thiols present in human hepatocytes may have cleaved SAM-760 to form benezenesulfinic acid.

TABLE 3

Geometric mean (% CV) and ratio of PK parameters after a single oral 5-mg dose of SAM-760 daily either alone or when coadministered with 400 mg ketoconazole daily

Treatment (N = 12)	C_{max}	$AUC_{0\text{-inf}}$
	ng/ml	ng/h per milliliter
SAM-760, 5 mg	3.43 (30)	154.5 (26)
SAM-760, 5 mg + ketoconazole, 400 mg	4.47 (20)	213.7 (18)
[SAM-760+Ketoconazole]/[SAM-760]	1.30	1.38

The key goal of the current post hoc investigation was to use in vitro tools to verify the observed CYP3A DDI of SAM-760 in the presence of ketoconazole. The in vitro data revealed that predominant metabolic pathway (~43%) in human hepatocytes was non-CYP mediated. The remaining radioactivity (Table 1) in human hepatocytes was sensitive to 1-ABT; therefore, enzyme phenotyping was performed in human hepatocytes by studying the formation of each of the 1-ABT–sensitive metabolites and their inhibition in the presence of isozyme-specific P450 inhibitors. The fraction of SAM-760 metabolized by each of the major P450 isozymes was calculated using eq. 1, 2, 3. 1-ABT–sensitive oxidative metabolites of SAM-760 were primarily formed from CYP3A, with minor contributions from other P450 isoforms CYP2C19 and CYP2D6. Using ketoconazole as the probe CYP3A inhibitor and using the in vitro human hepatocyte derived f_m CYP3A (33%), the static equation accurately predicted the observed ~1.38-fold change in the $AUC_{0\text{-inf}}$ of SAM-760.

This case study illustrates a post hoc investigation of [^{14}C]SAM-760 in human hepatocytes and verification of its observed clinical DDI. In conclusion, SAM-760 was predominantly cleared via a novel pathway of metabolism of the aryl sulfonamide group. This novel reaction proceeded nonenzymatically, via thiol-mediated reductive cleavage of the aryl sulfonamide yielding benzenesulfinic acid. Identification of this unexpected, non-P450–catalyzed reaction substantiates the use of human hepatocytes to study low-turnover compounds in the discovery and development stages. Although several methods have been validated and reviewed to study the metabolism of low-turnover compounds (Di et al., 2013; Di and Obach, 2015; Hutzler et al., 2015), this article emphasizes the importance of monitoring metabolite formation to accurately identify fractions of metabolism via both P450 and non-P450 pathways and to enable the assessment of DDI risks in clinical development. Finally, in vitro enzyme phenotyping studies of SAM-760 in human hepatocytes provided important insights into explaining the lower than predicted PK interaction of SAM-760 with ketoconazole.

Acknowledgments

We thank Douglas Spracklin and Jennifer Liras for support of the scientific investigations of this manuscript, and Michael Coutant for discussions on pharmaceutical properties of SAM-760. We also thank Andre Negahban for discussions and guidance on the metabolite quantification assay.

Authorship Contributions

Participated in research design: Sawant-Basak, Obach, Doran, Tse, and Comery.

Conducted experiments: Obach, Doran, Schildknegt, and Gao.

Contributed new reagents or analytic tools: Obach, Doran, Schildknegt, and Gao.

Performed data analysis: Sawant-Basak, Obach, Doran, Lockwood, Gao, Mancuso, Tse, and Comery.

Wrote or contributed to the writing of the manuscript: Sawant-Basak, Obach, Doran, Lockwood, Mancuso, and Tse.

References

Conroy CW, Schwam H, and Maren TH (1984) The nonenzymatic displacement of the sulfamoyl group from different classes of aromatic compounds by glutathione and cysteine. *Drug Metab Dispos* **12**:614–618.

Di L, Atkinson K, Orozco CC, Funk C, Zhang H, McDonald TS, Tan B, Lin J, Chang C, and Obach RS (2013) In vitro-in vivo correlation for low-clearance compounds using hepatocyte relay method. *Drug Metab Dispos* **41**:2018–2023.

Di L and Obach RS (2015) Addressing the challenges of low clearance in drug research. *AAPS J* **17**:352–357.

Foley AG, Hirst WD, Gallagher HC, Barry C, Hagan JJ, Upton N, Walsh FS, Hunter AJ, and Regan CM (2008) The selective 5-HT6 receptor antagonists SB-271046 and SB-399885 potentiate NCAM PSA immunolabeling of dentate granule cells, but not neurogenesis, in the hippocampal formation of mature Wistar rats. *Neuropharmacology* **54**:1166–1174.

Guest EJ, Rowland-Yeo K, Rostami-Hodjegan A, Tucker GT, Houston JB, and Galetin A (2011) Assessment of algorithms for predicting drug-drug interactions via inhibition mechanisms: comparison of dynamic and static models. *Br J Clin Pharmacol* **71**:72–87.

Haydar SN, Andrae PM, Yun H, and Robichaud AJ (2009) inventors, Wyeth LLC, assignee. 1-(Arylsulfonyl)-4-(piperazin-1-yl)-1H-benzimidazole compounds as 5-hydroxytryptamine-6 receptor ligands and their preparation and use in the treatment of diseases. U.S. patent 8,063,053 B2.

Hirst WD, Stean TO, Rogers DC, Sunter D, Pugh P, Moss SF, Bromidge SM, Riley G, Smith DR, Bartlett S, et al. (2006) SB-399885 is a potent, selective 5-HT6 receptor antagonist with cognitive enhancing properties in aged rat water maze and novel object recognition models. *Eur J Pharmacol* **553**:109–119.

Hutzler JM, Ring BJ, and Anderson SR (2015) Low-turnover drug molecules: a current challenge for drug metabolism scientists. *Drug Metab Dispos* **43**:1917–1928.

Kalgutkar AS, Jones R, and Sawant AD (2010) Sulfonamide as an essential functional group in drug design, in *Metabolism, Pharmacokinetics, and Toxicity of Functional Groups: Impact of Chemical Building Blocks on ADMET* (Smith DA ed) pp 210–275, Royal Society of Chemistry, Cambridge, UK.

Koeplinger KA, Zhao Z, Peterson T, Leone JW, Schwende FS, Heinrikson RL, and Tomasselli AG (1999) Activated sulfonamides are cleaved by glutathione-S-transferases. *Drug Metab Dispos* **27**:986–991.

Kotegawa T, Laurijssens BE, Von Moltke LL, Cotreau MM, Perloff MD, Venkatakrishnan K, Warrington JS, Granda BW, Harmatz JS, and Greenblatt DJ (2002) In vitro, pharmacokinetic, and pharmacodynamic interactions of ketoconazole and midazolam in the rat. *J Pharmacol Exp Ther* **302**:1228–1237.

Larsen JD and Bundgaard H (1989) Prodrug forms for the sulfonamide group. IV. Kinetics of hydrolysis of N-sulfonyl pseudourea derivatives. *Acta Pharm Nord* **1**:31–40.

Liu KG, Robichaud AJ, Greenfield AA, Lo JR, Grosanu C, Mattes JF, Cai Y, Zhang GM, Zhang JY, Kowal DM, et al. (2011) Identification of 3-sulfonylindazole derivatives as potent and selective 5-HT(6) antagonists. *Bioorg Med Chem* **19**:650–662.

Maher-Edwards G, Dixon R, Hunter J, Gold M, Hopton G, Jacobs G, Hunter J, and Williams P (2011) SB-742457 and donepezil in Alzheimer disease: a randomized, placebo-controlled study. *Int J Geriatr Psychiatry* **26**:536–544.

Rautio J, Vernerová M, Aufderhaar I, and Huttunen KM (2014) Glutathione-S-transferase selective release of metformin from its sulfonamide prodrug. *Bioorg Med Chem Lett* **24**:5034–5036.

Singh SK, Vobbalareddy S, Kalleda SR, Casturi SR, Mullangi R, Ramanujam R, Yeleswarapu KR, and Iqbal J (2006) N-acylated sulfonamide sodium salt: a prodrug of choice for the bifunctional 2-hydroxymethyl-4-(5-phenyl-3-trifluoromethyl-pyrazol-1-yl) benzenesulfonamide class of COX-2 inhibitors. *Bioorg Med Chem Lett* **16**:3921–3926.

Vuppugalla R, Zhang Y, Chang S, Rodrigues AD, and Marathe PH (2012) Impact of nonlinear midazolam pharmacokinetics on the magnitude of the midazolam-ketoconazole interaction in rats. *Xenobiotica* **42**:1058–1068.

Zhao Z, Koeplinger KA, Peterson T, Conradi RA, Burton PS, Suarato A, Heinrikson RL, and Tomasselli AG (1999) Mechanism, structure-activity studies, and potential applications of glutathione S-transferase-catalyzed cleavage of sulfonamides. *Drug Metab Dispos* **27**:992–998.

Address correspondence to: Dr. Aarti Sawant-Basak, Pharmacokinetics, Dynamics, and Metabolism, Worldwide Research and Development, Pfizer Inc., 1 Portland Street, Kendall Square, Cambridge, MA 02139. E-mail: aarti.sawant@pfizer.com